PHYSICAL REVIEW B **87**, 060402(R) (2013)

Exact asymptotic behavior of magnetic stripe domain arrays

Tom H. Johansen,[1,2,3] Alexey V. Pan,[3] and Yuri M. Galperin[1,2,4,5]

[1]*Department of Physics, University of Oslo, 0316 Oslo, Norway*

[2]*Center for Advanced Study at the Norwegian Academy of Science and Letters, 0271 Oslo, Norway*

[3]*Institute for Superconducting and Electronic Materials, University of Wollongong, Northfields Avenue, Wollongong, NSW 2522, Australia*

[4]*Physico-Technical Institute RAS, 194021 St. Petersburg, Russian Federation*

[5]*Argonne National Laboratory, 9700 S. Cass Ave., Lemont, Illinois 60439, USA*

(Received 5 November 2012; published 4 February 2013)

The classical problem of magnetic stripe domain behavior in films and plates with uniaxial magnetic anisotropy is addressed. Exact analytical results are derived for the stripe domain widths as a function of applied perpendicular field H, in the regime where the domain period becomes large. The stripe period diverges as $(H_c - H)^{-1/2}$, where H_c is the critical (infinite period) field, an exact result confirming a previous conjecture. The magnetization approaches saturation as $(H_c - H)^{1/2}$, a behavior that compares excellently with experimental data obtained for a 4-μm thick ferrite garnet film. The exact analytical solution provides a new basis for precise characterization of uniaxial magnetic films and plates, illustrated by a simple way to measure the domain wall energy. The mathematical approach is applicable for similar analysis of a wide class of systems with competing interactions where a stripe domain phase is formed.

DOI: 10.1103/PhysRevB.87.060402 PACS number(s): 75.60.Ch, 75.70.Kw

Systems with competing interactions, in particular those with short-range attractive and long-range repulsive interactions, commonly develop modulations in the order parameter and form domain structures often consisting of a stripe pattern.[1,2] Realizations are found in a wide variety of systems, such as magnetic films and plates with uniaxial anisotropy,[3] magnetic liquids,[4,5] type-I superconductors in the intermediate state,[6,7] doped Mott insulators,[8] quantum Hall structures,[9,10] and monomolecular amphiphilic ("Langmuir") films.[11,12]

The uniaxial magnetic films, where ferrite garnets is a classical material studied extensively decades ago for use in bubble memory devices,[13,14] may be regarded as a prototype system for stripe domain behavior. Recently, the dynamical behavior of the domains in thick garnet films showed a vast potential for manipulation of micrometer-sized superparamagnetic beads dispersed in a water layer covering the film. By applying magnetic fields with oscillating in- and out-of-plane components, new principles for micromachines like colloidal ratchets, size separators, micro-tweezers, stirrers, etc., were demonstrated.[15–18] Moreover, it has been shown that the magnetic stripe domain structure, when placed adjacent to type-II superconductors, can strongly interact with the vortex matter, both in a manipulative way[19–21] and as a method to enhance flux pinning in the superconductor.[22–24] Thus one sees today considerable renewed interest in the collective behavior of magnetic stripe domains.

On the theoretical side, the treatment of magnetic domains in plates with perpendicular easy-axis anisotropy placed in an external magnetic field is challenging. Even solving the magnetostatic problem of one isolated linear stripe surrounded by reverse magnetization turned out rather complicated analytically, and for a regular array of alternating stripes, results were so far obtained only by numerical calculations.[25,26] In this work, based on the wall-energy model,[3] i.e., assuming domains separated by infinitely thin walls oriented normal to the plate, we derive an exact analytical solution for the behavior of a periodic array of interacting stripe domains in increasing applied field.

Consider a uniaxial plate of arbitrary thickness, t, where magnetic domains form a periodic lattice of parallel stripes with alternating magnetization $\pm M_s$, see Fig. 1. In an applied perpendicular field H the domains magnetized parallel and antiparallel to the field are characterized by their respective widths $a_\uparrow$ and $a_\downarrow$, and the magnetization of the plate is $M = M_s(a_\uparrow - a_\downarrow)/a$, where $a = a_\uparrow + a_\downarrow$ is the period of the stripe lattice.

Following the analysis of Kooy and Enz,[3] the energy density has three contributions: (i) the cost of forming domain walls, characterized by the energy σ_w per unit wall area, (ii) the energy gain of aligning the magnetization with the applied field, $-\mu_0 H M$, and (iii) the self-energy of the domain structure (demagnetization energy). The total energy, U, per unit volume of the plate can then be written as[13]

$$\frac{U(m,a)}{\mu_0 M_s^2} = 2\Lambda\frac{t}{a} - mh + \frac{1}{2}m^2 + 2\frac{a}{t}\sum_{n=1}^{\infty}\frac{\sin^2[n\pi(1+m)/2]}{(n\pi)^3}\left(1 - \mathrm{e}^{-n2\pi t/a}\right). \quad (1)$$

Here, $m = M/M_s$, $h = H/M_s$, and $\Lambda = \lambda/t$ where $\lambda = \sigma_w/\mu_0 M_s^2$ is a characteristic length. The equilibrium magnetization and stripe period at a given applied field is given by $\partial U/\partial m = \partial U/\partial a = 0$ and expressed by the two equations:

$$1 - 2x - \frac{2}{\pi}\mathcal{F}(2\pi x, 2\pi y) = h, \quad (2)$$

$$\mathcal{G}(2\pi x, 2\pi y) = 2\pi\Lambda. \quad (3)$$

Here, $x \equiv a_\downarrow/a = (1-m)/2$ and $y \equiv t/a$ and

$$\mathcal{F}(x,y) \equiv \sum_{n=1}^{\infty}\frac{\sin nx}{n^2}\,\frac{1-e^{-ny}}{y}, \quad (4)$$

$$\mathcal{G}(x,y) \equiv 8\sum_{n=1}^{\infty}\frac{\sin^2(nx/2)}{n^3}\,\frac{1-(1+ny)e^{-ny}}{y^2}. \quad (5)$$

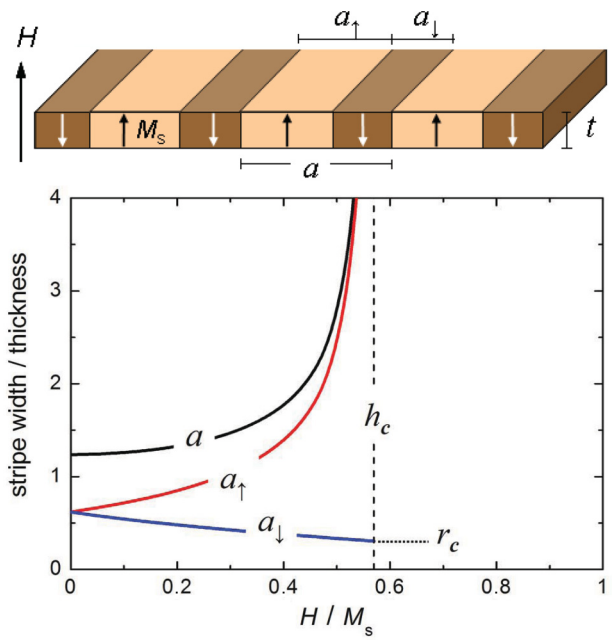

FIG. 1. (Color online) Cross section of a plate with magnetic stripe domain pattern (top) and numerical results for the domain widths as a function of the applied field for the case $\Lambda = 0.05$ (bottom).

The particular choice of new variables is motivated by the numerical solution of the problem shown graphically in the lower panel of Fig. 1 only for reference. The striking feature is that when the applied field approaches a critical value, $H_c = h_c M_s$ where $h_c < 1$, both the period a of the domain lattice and the width $a_\uparrow$ of the domains magnetized parallel to the field will diverge, whereas the reverse domains contract only moderately and terminate at a finite width $a_{\downarrow c}$. At fields above H_c, the material remains single-domain. In the new variables, the approach towards the critical values corresponds to both $x, y \to 0$, while the ratio $r \equiv x/y = a_\downarrow/t$ remains finite.[27]

Focus of the present analysis is to determine analytically the exact behavior as the field approaches the critical value. We first derive the relation between h_c and $a_{\downarrow c}$. For this, we introduce the auxiliary function $p_k(z) \equiv \sum_{n=1}^{\infty} n^{-(k+1)}\, \mathrm{e}^{-nz} =$ polylog$(k,-z)$ and write

$$\mathcal{F}(x,y) = \mathrm{Im}[p_1(-ix) - p_1(y - ix)]/y. \tag{6}$$

For small $|z|$, one has

$$p_1(z) = (\pi^2/6) + z(\ln z - 1) - (z^2/4) + (z^3/72) + \cdots, \tag{7}$$

which results in the following series expansion:

$$\mathcal{F}(x,y) = \arctan\left(\frac{x}{y}\right) + \frac{x}{y}\ln\sqrt{1+\frac{y^2}{x^2}} - \frac{x}{2} + \frac{xy}{24} + \frac{2yx^3 - xy^3}{2880} + \cdots. \tag{8}$$

Inserted in Eq. (2), it takes the form

$$h = 1 - \frac{2}{\pi}[\arctan(r) + r\ln\sqrt{1+r^{-2}}] - \frac{\pi}{3r}x^2 + \frac{\pi^3}{90r}(2 - r^{-2})x^4 + \cdots. \tag{9}$$

The critical field is therefore given by

$$h_c = \frac{2}{\pi}\arctan\left(r_c^{-1}\right) - \frac{r_c}{\pi}\ln\left(1 + r_c^{-2}\right), \tag{10}$$

where $r_c = a_{\downarrow c}/t$ is the critical, i.e., the terminal width of the minority (antiparallel to **H**) domains.

To find a relation between r_c and the material parameter Λ, a similar treatment is given to Eq. (3), using that $\mathcal{G}(x,y)$ can be expressed as a combination of the real parts of both $p_1(z)$ and $p_2(z)$ with complex arguments like those in Eq. (6). For small $|z|$, one has

$$p_2(z) = \zeta(3) - \frac{\pi^2 z}{6} + \frac{(3 - 2\ln z)z^2}{4} + \frac{z^3}{12} - \frac{z^4}{288} + \cdots, \tag{11}$$

where $\zeta(n)$ is the Riemann zeta-function, and Eq. (3) becomes

$$\ln(1+r^2) + r^2\ln(1+r^{-2}) - \frac{\pi^2}{3}x^2 - \frac{\pi^4}{270}(3 - 9r^{-2} + r^{-4})x^4 + \cdots = 2\pi\Lambda. \tag{12}$$

The terminal width of the minority domains is therefore given by

$$\ln\left(1 + r_c^2\right) + r_c^2\ln\left(1 + r_c^{-2}\right) = 2\pi\Lambda, \tag{13}$$

and is shown graphically in Fig. 2. The figure also shows the dependence $h_c(\Lambda)$, which follows from Eqs. (10) and (13). Both these curves, if replotted as functions of Λ^{-1}, agree excellently with the numerical solutions presented in Fig. 7 of the Ref. 25. Note that for any material, i.e., given σ_w and M_s, the critical field decreases with Λ, and for $\Lambda > 0.2$

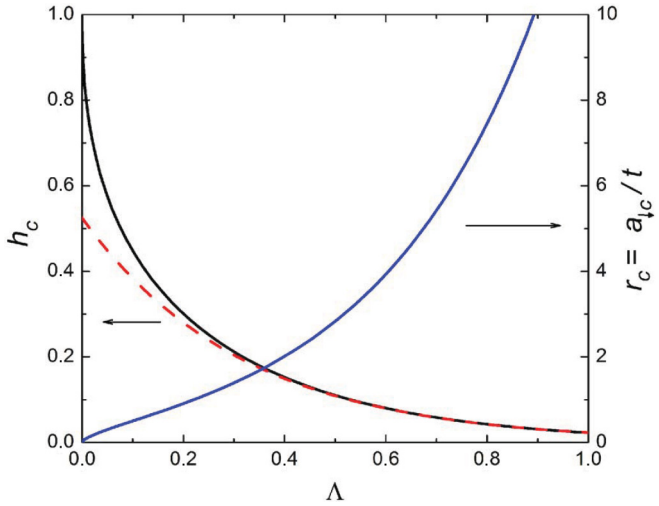

FIG. 2. (Color online) The critical field, $h_c = H_c/M_s$, and terminal minority domain width r_c as functions of $\Lambda = \sigma_w/(\mu_0 M_s^2 t)$. The dashed line represents $h_c(\Lambda) = (\sqrt{\mathrm{e}}/\pi)\exp(-\pi\Lambda)$.

this dependence rapidly approaches $h_c = (\sqrt{e}/\pi)\exp(-\pi\Lambda)$, shown as a dashed line in Fig. 2.

Consider next the behavior in the vicinity of $h = h_c$. Expanding Eqs. (9) and (12) in Taylor series around the critical point, one finds to the lowest order that $\pi x^2 = 2r_c(h_c - h)$. It then follows that the stripe pattern period, $a/t = r/x$, diverges according to

$$\frac{a}{t} = \sqrt{\frac{\pi r_c}{2}}\,(h_c - h)^{-1/2}. \tag{14}$$

At the same time, the reverse domain approaches its terminal width as

$$\frac{a_\downarrow}{t} = r_c + \frac{\pi(h_c - h)}{3\,\ln\left(1 + r_c^{-2}\right)}, \tag{15}$$

and the magnetization, $m = 1 - 2rt/a$, approaches saturation according to

$$m = 1 - \sqrt{\frac{8r_c}{\pi}}(h_c - h)^{1/2}. \tag{16}$$

To compare the analytical results with the quantitative behavior of a typical sample with magnetic stripe domains, we prepared a film of bismuth-substituted ferrite garnet, $(Y,Lu,Bi)_3(FeGa)_5O_{12}$, by liquid phase epitaxial growth on a (111) oriented gadolinium gallium garnet (GGG) substrate. Oxide powders of the constituent rare earths, bismuth, iron and gallium, as well as PbO and B_2O_3, were initially melted in a thick-walled platinum crucible. To ensure homogeneity of the solution, a stirrer mixed the melt while being kept in the three-zone resistive furnace at 1050 °C for 30 minutes. Prior to the film growth the melt temperature was reduced to 700 °C. The GGG wafer was mounted horizontally in a three-finger platinum holder attached to a shaft rotating by 60 rpm and brought slowly down towards the melt. Finally, the substrate was dipped into the melted for 8 minutes resulting in a macroscopically uniform ferrite garnet film (FGF) grown on one side of the substrate, see Ref. 28 for more details. A nearly square plate of area $A = 21$ mm^2 was selected for measurements. The thickness of the FGF was determined by viewing the sample edge-on in a scanning electron microscope, where a sharp contrast between the film and the substrate becomes visible. The ferrite garnet thickness was $t = (4.0 \pm 0.2)\ \mu$m.

Shown in Fig. 3 is the result of dc-magnetization measurements performed using a Quantum Design Magnetic Property Measurement System (SQUID magnetometer) with the FGF mounted perpendicular to the applied field. Above the field of 17 kA/m, the data show linear increase, which is due to the paramagnetic substrate, in combination with the FGF being single domain having a constant moment. The fitted straight line intersects the vertical axis at a point which determines the saturation moment of the FGF sample, $\mu_s = 2.9110^{-6}$ Am^2, which corresponds to $M_s = 34.6$ kA/m.

Figure 4 shows the reduced magnetic moment of the FGF obtained by subtracting the paramagnetic background from the raw data. Based on the model result (16), the reduced magnetization was fitted to the predicted asymptotic form $(H_c - H)^{1/2}$ using data over a field range below the point where the moment saturates. The best linear fit of the reduced moment squared is

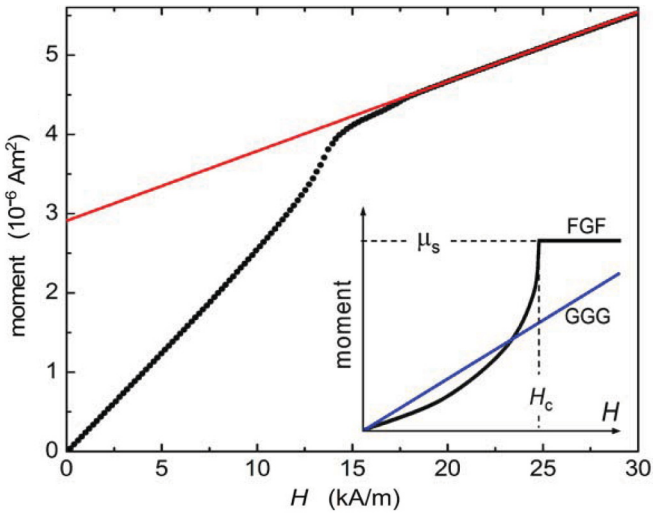

FIG. 3. (Color online) Magnetic moment of a ferrite garnet film vs applied perpendicular field. The straight line represents the contribution from the paramagnetic GGG substrate. The inset shows a schematic of the two contributions to the moment.

seen in the upper inset, from which we find a critical field of $H_c = 13.9$ kA/m, and thus $h_c = 0.40$. It follows then from Eq. (10) that $r_c = 0.605$, and from Eq. (13) one finds $\Lambda = 0.126$, and $\lambda = 0.126t = 0.504$ microns. The specific wall energy has therefore the value $\sigma_w = 7.58 \cdot 10^{-4}$ J/m^2.

In previous analyses of the stripe domain problem, see, e.g., Ref. 26, it was suggested that as the applied field approaches h_c, the stripe period diverges with a power $\beta \approx 0.5$. In this work, it has been shown that $\beta = 1/2$ is an exact result. Consider next what is the field range over which the asymptotic behavior is expected to be observed. There are previous works[25] where experimental data were fitted by numerical M-H curves approaching saturation seemingly with a finite slope. Furthermore, in the classical book Ref. 13, the Fig. 2.3

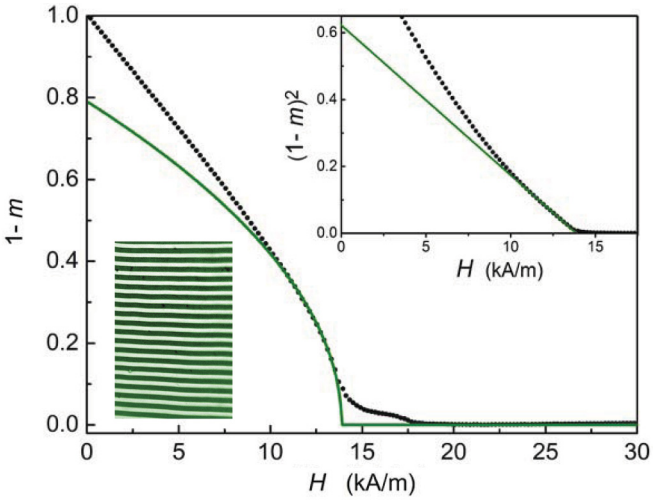

FIG. 4. (Color online) Reduced magnetization $(M_s - M)/M_s$, experimental data and fitted model behavior, Eq. (13), vs applied magnetic field. (Upper inset) The linear fit to the reduced magnetization squared. (Lower inset) Magnetooptical image showing that the FGF sample displays a parallel stripe domain pattern.

shows M-H curves approaching saturation with a finite slope strongly depending on the sample thickness. To resolve this apparent inconsistency, we analyzed the Eqs. (9) and (12) up to the next order, i.e., expanding them to $(r - r_c)^2$ and keeping the terms $\propto x^4$. The analysis shows that Eqs. (14)–(16) provide a good description as long as

$$(h_c - h) \lesssim \min\{r_c, 1\}. \tag{17}$$

Thus, for thick plates, $t \gg \lambda$, one has a very small $2\pi\Lambda$ and $r_c \approx [2\pi\Lambda/\ln(1/2\pi\Lambda)]^{1/2}$, which is much less than unity. Thus it follows that the asymptotic behavior (16) will be observed only very close to h_c. In practice, the field interval may be beyond experimental resolution, and the slope of the magnetization curve near $h = h_c$ appears finite. For thinner plates and films, r_c rapidly increases, see Fig. 2, and the inequality (17) becomes much weaker, and the range where one should observe the critical behavior Eq. (16) will be sizable, as demonstrated in the present experiments.

Note also the presence of a small shoulder in the reduced magnetization data in Fig. 4 seen just above H_c. Here, the behavior deviates significantly from the model prediction, and is caused by topological fluctuations in the domain pattern. The role of material defects causing wall pinning becomes significant, and the stripes lose their alignment, a scenario which is readily seen visually by following the behavior using magnetooptical imaging.[29]

Finally, consider the stripe behavior at small fields. As evident from Eq. (2), the solution for $h = 0$ is $x = 1/2$ for any y. Expanding the function $\mathcal{F}$ in powers of $x - 1/2$, and keeping only the lowest order term, one gets from Eq. (2) that $m = \chi h$, where the susceptibility is given by

$$\chi = \pi y_0 / \ln\cosh(\pi y_0). \tag{18}$$

Here, y_0 is the solution of Eq. (3) for $x = 1/2$, i.e., $\mathcal{G}(\pi, 2\pi y_0) = 2\pi\Lambda$, which defines the low-field stripe period in terms of the material parameters.

In summary, we have presented an analytical asymptotic solution to the problem of modeling the behavior of an infinite array of parallel alternating magnetic stripe domains subjected to a transverse field. The mathematical approach used in this work can be applied to derive exact results also for other systems[4,30,31] where stripe domain phases are formed and described by a configurational energy term similar to the one treated in the present case.

The work was financially supported by the Australian Research Council International Linkage Project LX0990073 and Discovery Project DP0879933 and the Norwegian Research Council. T.H.J. acknowledges also the partial funding by the Brazilian national research council (CNPq), Project 401294/2012-9, which is part of the "Science without Borders" program. Y.G. is grateful to I. Lukyanchuk and A. Mel'nikov for discussions.

[1] M. Seul and D. Adelman, Science **267**, 476 (1995).
[2] C. Sagui, E. Asciutto, and C. Roland, Nano Lett. **5**, 389 (2005).
[3] C. Kooy and U. Enz, Philips Res. Rep. **15**, 7 (1960).
[4] C. Flament, J.-C. Bacri, A. Cebers, F. Elias, and R. Perzynski, Europhys. Lett. **34**, 225 (1996).
[5] M. F. Islam, K. H. Lin, D. Lacoste, T. C. Lubensky, and A. G. Yodh, Phys. Rev. E **67**, 021402 (2003).
[6] R. P. Huebener, *Magnetic Flux Structures of Superconductors* (Springer-Verlag, New York, 2001).
[7] R. Prozorov, Phys. Rev. Lett. **98**, 257001 (2007).
[8] J. M. Tranquada, B. J. Sternlieb, J. D. Axe, Y. Nakamura, and S. Uchida, Nature (London) **375**, 561 (1995).
[9] M. M. Fogler, A. A. Koulakov, and B. I. Shklovskii, Phys. Rev. B **54**, 1853 (1996).
[10] A. A. Koulakov, M. M. Fogler, and B. I. Shklovskii, Phys. Rev. Lett. **76**, 499 (1996).
[11] P. G. De Gennes and C. Taupin, J. Phys. Chem. **86**, 2294 (1982).
[12] W. M. Gelbart and A. Ben-Shaul, J. Phys. Chem. **100**, 13169 (1996).
[13] A. H. Bobeck and E. Della Torre, *Magnetic Bubbles* (American Elsevier, New York, 1975).
[14] A. P. Malozemoff and J. C. Slonczewski, *Magnetic Domain Walls in Bubble Materials* (Academic Press, New York, 1979).
[15] L. E. Helseth, T. M. Fischer, and T. H. Johansen, Phys. Rev. Lett. **91**, 208302 (2003).
[16] L. E. Helseth, L. E. Wen, R. W. Hansen, T. H. Johansen, P. Heinig, and T. M. Fischer, Langmuir **20**, 7323 (2004).
[17] P. Tierno, T. H. Johansen, and Th. M. Fischer, Phys. Rev. Lett. **99**, 038303 (2007).
[18] P. Tierno, Th. M. Fischer, T. H. Johansen, and F. Sagues, Phys. Rev. Lett. **100**, 148304 (2008).
[19] P. E. Goa, H. Hauglin, A. A. F. Olsen, D. V. Shantsev, and T. H. Johansen, Appl. Phys. Lett. **82**, 79 (2003).
[20] L. E. Helseth, P. E. Goa, H. Hauglin, M. Baziljevich, and T. H. Johansen, Phys. Rev. B **65**, 132514 (2002).
[21] J. I. Vestgården, D. V. Shantsev, A. A. F. Olsen, Y. M. Galperin, V. V. Yurchenko, P. E. Goa, and T. H. Johansen, Phys. Rev. Lett. **98**, 117002 (2007).
[22] V. H. Dao, S. Burdin, and A. Buzdin, Phys. Rev. B **84**, 134503 (2011).
[23] M. Iavarone, A. Scarfato, F. Bobba, M. Longobardi, G. Karapetrov, V. Novosad, V. Yefremenko, F. Giubileo, and A. M. Cucolo, Phys. Rev. B **84**, 024506 (2011).
[24] V. Vlasko-Vlasov, A. Buzdin, A. Melnikov, U. Welp, D. Rosenmann, L. Uspenskaya, V. Fratello, and W. Kwok, Phys. Rev. B **85**, 064505 (2012).
[25] J. A. Cape and G. W. Lehman, J. Appl. Phys. **42**, 5732 (1971).
[26] K. L. Babcock and R. M. Westervelt, Phys. Rev. A **40**, 2022 (1989).
[27] From Eqs. (2) and (3), it is not evident that such a critical point should exist. Our choice of variables was made by postulating an h_c where a diverges and $a_\downarrow$ remains finite (as suggested by numerics) and realizing that the leading terms in the analytical functions representing the Fourier sums depend only on x/y as $x, y \to 0$.
[28] L. E. Helseth, A. G. Solovyev, R. W. Hansen, E. I. Il'yashenko, M. Baziljevich, and T. H. Johansen, Phys. Rev. B **66**, 064405 (2002).
[29] P. E. Goa, H. Hauglin, A. A. F. Olsen, M. Baziljevich, and T. H. Johansen, Rev. Sci. Instrum. **74**, 141 (2003).
[30] R. E. Goldstein, D. P. Jackson, and A. T. Dorsey, Phys. Rev. Lett. **76**, 3818 (1996).
[31] A. T. Dorsey and R. E. Goldstein, Phys. Rev. B **57**, 3058 (1998).